

RESONANT PRODUCTION OF COLOR OCTET ELECTRON AT THE LHeC

M. SAHIN*

TOBB University of Economics and Technology, Physics Division, Ankara, Turkey

S. SULTANSOY†

TOBB University of Economics and Technology,

Physics Division, Ankara, Turkey and

Institute of Physics, National Academy of Sciences, Baku, Azerbaijan

S. TURKOZ‡

Ankara University, Department of Physics, Ankara, Turkey

Abstract

In composite models with colored preons leptogluons (l_8) has a same status with leptoquarks, excited leptons and quarks etc. We analyze resonant production of color octet electron (e_8) at QCD Explorer stage of the Large Hadron electron Collider (LHeC). It is shown that the e_8 discovery at the LHeC simultaneously will determine the compositeness scale.

*Electronic address: m.sahin@etu.edu.tr

†Electronic address: ssultansoy@etu.edu.tr

‡Electronic address: turkoz@science.ankara.edu.tr

I. INTRODUCTION

A large number of “fundamental” particles, as well as observable free parameters (put by hand), in Standard Model (SM) indicate that it is not “the end of story”. Physics has met similar situation two times in the past: one is the Periodic Table of the Elements which was clarified by Rutherford’s experiment later, the other is hadron inflation which has resulted in quark model. This analogy implies the preonic structure of the SM fermions (see [1] and references therein). The preonic models predict a zoo of new particles such as excited leptons and quarks, leptoquarks, leptogluons etc. Excited fermions and leptoquarks are widely discussed in literature and their searches are inseparable parts of future collider’s physics programs. Unfortunately, leptogluons did not attract necessary attention, while they are predicted in all models with colored preons (see, for example, [2], [3], [4], [5], [6], [7]).

Lower bound on leptogluon masses, 86 GeV, given in PDG [8] reflects twenty years old Tevatron results [9]. As mentions in [10] D0 clearly exclude 200 GeV leptogluons and could naively place the constraint $M_{LG} \gtrsim 325$ GeV. Fifteen years old H1 results on color octet electron, e_8 , search [11] has excluded the compositeness scale $\Lambda \lesssim 3\text{TeV}$ for $M_{e8} \simeq 100$ GeV and $\Lambda \lesssim 240$ GeV for $M_{e8} \simeq 250$ GeV. The advantage of lepton-hadron colliders is the resonant production of leptogluons, whereas at hadron and lepton colliders they are produced in pairs.

The sole realistic way to TeV scale in lepton-hadron collisions are presented by linac-ring type electron-proton colliders (see reviews [12], [13], [14] and references therein). Recently CERN, ECFA and NuPECC initiated the study on the LHC based ep colliders [15]. Two options are considered for the Large Hadron electron Collider (LHeC): the construction of new e-ring in the LHC tunnel [16] or the construction of e-linac tangentially to the LHC [17], [18], [19]. It should be noted that energy of electrons in first option is limited by synchrotron radiation, whereas in second option energy of electrons can be increased by lengthening the linac. Tentative parameters for linac-ring options of the LHeC are presented in the Table 1. QCD Explorer stage(s) is mandatory: it will provide necessary information on PDF’s for adequate interpretation of future LHC results and it will clarify QCD basics, as well. The realization of the Energy Frontier stage(s) will be determined by the LHC results on Beyond the Standard Model (BSM) physics.

Stage	E_e, GeV	\sqrt{s}, TeV	$L, 10^{32} \text{cm}^{-2} \text{s}^{-1}$
LHeC/QCDE-1	70	1.4	1 – 10
LHeC/QCDE-2	140	1.98	1 – 10
LHeC/EF	500	3.74	1

Table I: Tentative parameters of the LHeC linac-ring options. QCDE and EF denotes QCD Explorer and Energy Frontier, respectively.

In this paper we investigate potential of QCDE stages of the LHeC in search for color octet electron via resonant production. In section 2, Lagrangian for e_8 interactions is presented and it's decay widths and production cross sections at different stages of LHeC are evaluated. Section 3 is devoted to detailed analysis of leptogluon signatures at QCD-E stages of the LHeC. Finally, concluding remarks are given in section 4.

II. INTERACTION LAGRANGIAN, DECAY WIDTH AND PRODUCTION CROSS SECTION

For the interaction of leptogluons with corresponding lepton and gluon we use the following Lagrangian [8], [20]:

$$L = \frac{1}{2\Lambda} \sum_l \{ \bar{l}_8^\alpha g_s G_{\mu\nu}^\alpha \sigma^{\mu\nu} (\eta_L l_L + \eta_R l_R) + h.c. \} \quad (1)$$

where $G_{\mu\nu}^\alpha$ is field strength tensor for gluon, index $\alpha = 1, 2, \dots, 8$ denotes the color, g_s is gauge coupling, η_L and η_R are the chirality factors, l_L and l_R denote left and right spinor components of lepton, $\sigma^{\mu\nu}$ is the anti-symmetric tensor and Λ is the compositeness scale. The leptonic chiral invariance implies $\eta_L \eta_R = 0$. For numerical calculations we add leptogluons into the CalcHEP program [21].

Decay width of the color octet electron is given by

$$\Gamma_{e8} = \frac{\alpha_s M_{e8}^3}{4\Lambda^2} \quad (2)$$

In Fig. 1 decay widths of leptogluons are presented for two scenarios, $\Lambda = M_{e8}$ and $\Lambda = 10 \text{ TeV}$.

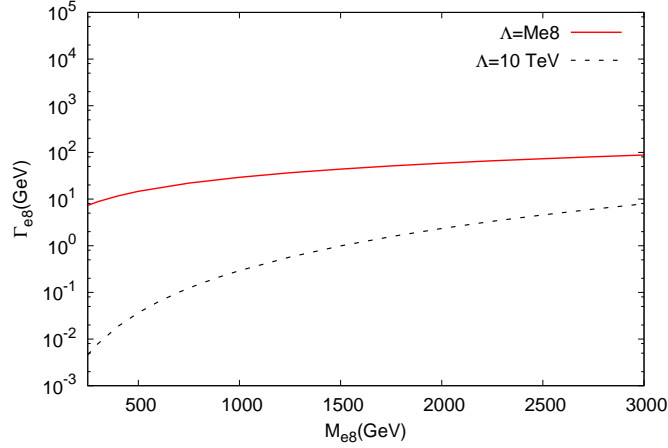


Figure 1: Leptogluon decay width via its mass for $\Lambda = M_{e8}$ and $\Lambda = 10$ TeV.

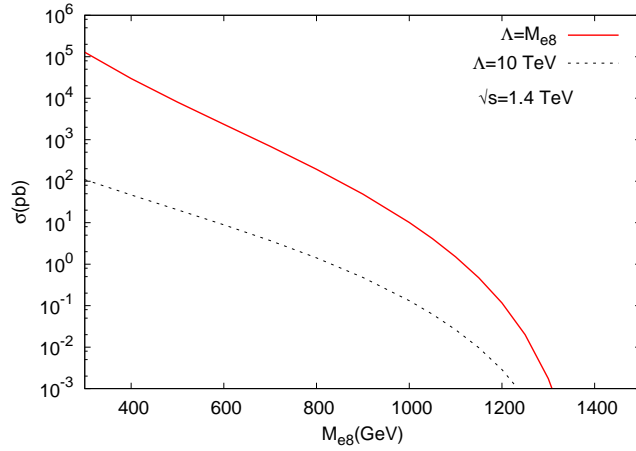


Figure 2: Resonant e_8 production at the LHeC/QCDE-1.

The resonant e_8 production cross sections for there stages at the LHeC from Table 1, evaluated using CalcHEP with CTEQ6L parametrization [22] for parton distribution functions, are presented in Figs. 2-4. It is seen that sufficiently high cross-sections allow the exploration of the e_8 mass range almost up to the kinematical limits.

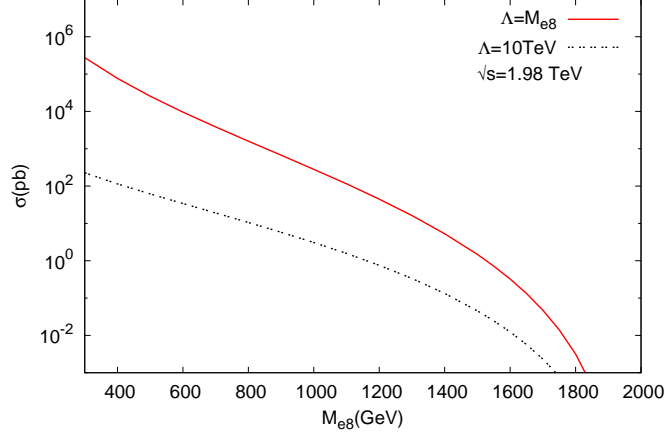


Figure 3: Resonant e_8 production at the LHeC/QCDE-2.

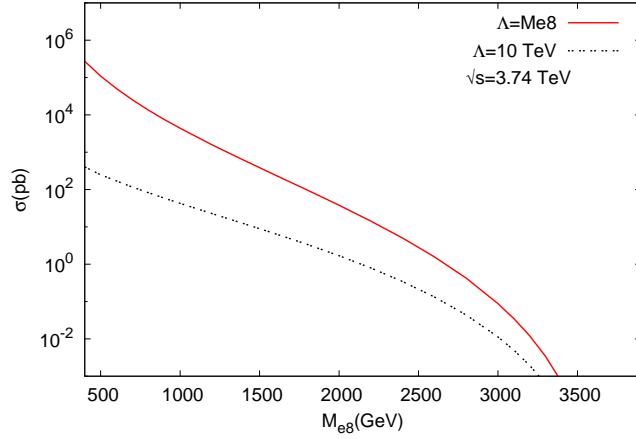


Figure 4: Resonant e_8 production at the LHeC/EF.

III. SIGNAL AND BACKGROUND ANALYSIS

A. LHeC/QCDE-1 stage

First of all, let us consider p_T and η distributions for signal and background processes in order to determine appropriate kinematical cuts. Transverse momentum distribution of final state jets for signal at $\Lambda = 10$ TeV and background is shown in Fig. 5. It is seen that $p_T > 150$ GeV cut essentially reduces background, whereas signal is almost unaffected. Figs. 6 and 7 represent pseudo-rapidity (η) distributions for electrons and jets, respectively. As seen from figure 7, η_e -distribution for signal and background are not drastically different.

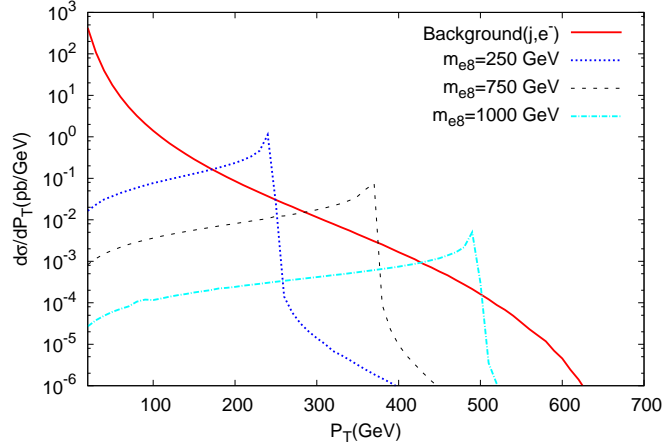


Figure 5: Transverse momentum distributions of final state jets for signal and background at $\sqrt{s} = 1.4$ TeV and $\Lambda = 10$ TeV.

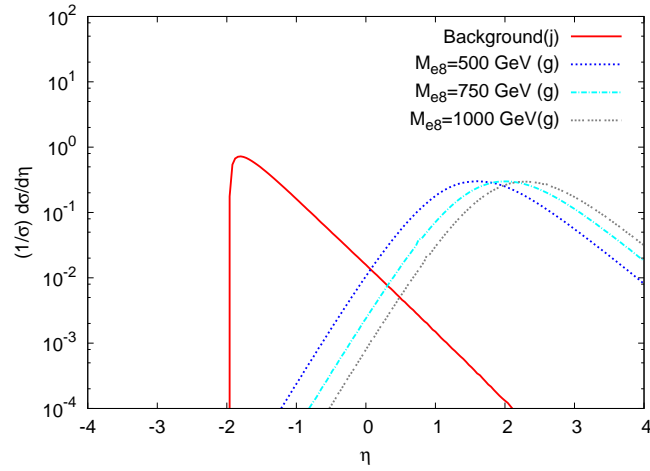


Figure 6: Pseudo-rapidity distributions of jets for signal and background at $\sqrt{s} = 1.4$ TeV and $\Lambda = 10$ TeV.

Concerning η_j , most of signal lies above $\eta = 0$, whereas 99 % of background is concentrated in $-2 < \eta_j < 0$ region. For this reasons below we use $p_T > 150$, $|\eta_e| < 4$ and $0 < \eta_j < 4$. With these cuts we present in Fig. 8 invariant mass distributions for signal and background.

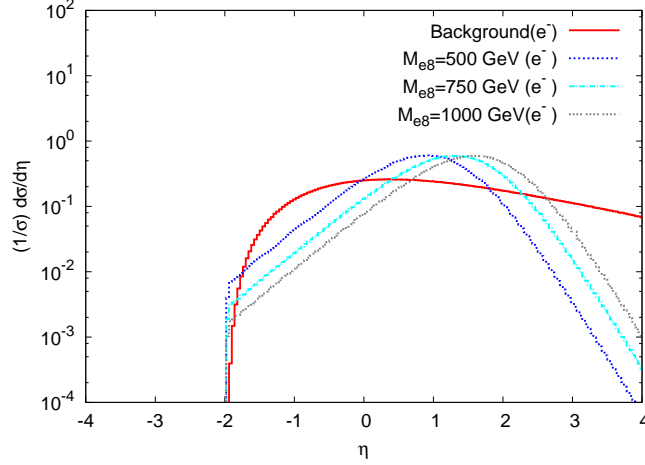


Figure 7: Pseudo-rapidity distributions of electrons for signal and background at $\sqrt{s} = 1.4$ TeV and $\Lambda = 10$ TeV.

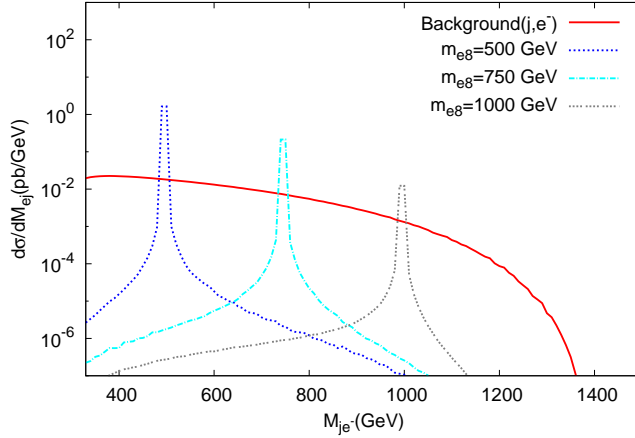


Figure 8: ej invariant mass distributions for signal and background at $\sqrt{s} = 1.4$ TeV and $\Lambda = 10$ TeV.

Advantage of resonant production will provide an opportunity to probe compositeness scale will above the center of mass energy of the collider. For statistical significance we use following formula:

$$SS = \frac{S}{\sqrt{S+B}} \quad (3)$$

where S and B denote number of signal and background events, respectively.

Numbers of signal and background events for different M_{e8} values are presented in Table 2 for $L_{int} = 1fb^{-1}$. In calculating these values, in addition to cuts given above, we have

M_{e8} , GeV	$\Lambda = M_{e8}$		$\Lambda = 10$ TeV	
	S	B	S	B
500	1.1×10^7	1.1×10^3	3.3×10^4	700
750	6.4×10^5	630	4.2×10^3	280
1000	2.2×10^4	165	250	53
1250	81	6	1	1

Table II: Number of signal and background events for LHeC/QCDE-1 with $L_{int} = 1fb^{-1}$.

M_{e8} , GeV	$L_{int} = 1fb^{-1}$	$L_{int} = 10fb^{-1}$
500	150 (200)	275 (350)
750	65 (90)	125 (160)
1000	22 (30)	45 (58)

Table III: Achievable compositeness scale (Λ in TeV units) at LHeC/QCDE-1 for 5σ (3σ) statistical significance.

used mass windows as $M_{e8} - 2\Gamma_{e8} < M_{ej} < M_{e8} + 2\Gamma_{e8}$ for $\Gamma_{e8} > 10$ GeV and $M_{e8} - 20$ GeV $< M_{ej} < M_{e8} + 20$ GeV for $\Gamma_{e8} < 10$ GeV. It is seen that resonant production of color octet electron will provide very clean signature for masses up to $M_{e8} \simeq 1\text{TeV}$.

In Table 3 we present reachable compositeness scale values for $L_{int} = 1$ and $L_{int} = 10fb^{-1}$. It is seen that multi-hundred TeV scale can be searched for $M_{e8} = 500$ GeV. Then, increase of the luminosity by one order results in two times higher values for Λ .

Lastly, for a given $L_{int} = 1fb^{-1}$, the upper mass limits for 5σ discovery at LHeC/QCDE-1 stage are $M_{e8} = 1100$ GeV and $M_{e8} = 1275$ GeV for $\Lambda = 10$ TeV and $\Lambda = M_{e8}$, respectively.

B. LHeC/QCDE-2 stage

In order to determine corresponding cuts we present p_T , η_j and η_e distributions for signal and background processes in Figs 9, 10 and 11, respectively. The figures indicate that significant change takes place only for η_j . In this subsections we will use $p_T > 150$, $|\eta_e| < 4$ and $-0.5 < \eta_j < 4$. The invariant mass distributions obtained with this cuts are given in Fig. 12.

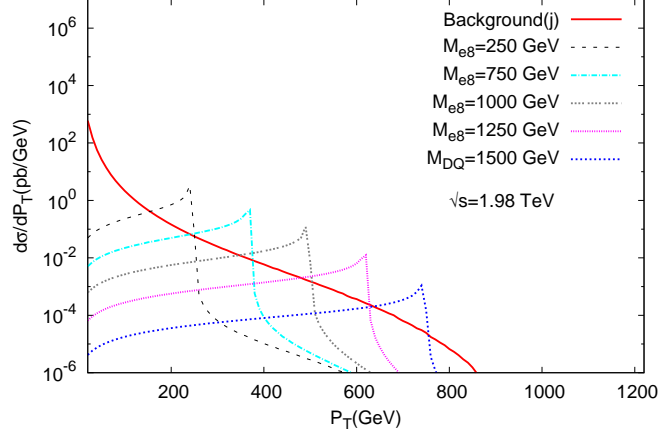


Figure 9: Transverse momentum distributions of final state jets for signal and background at $\sqrt{s} = 1.98$ TeV and $\Lambda = 10$ TeV.

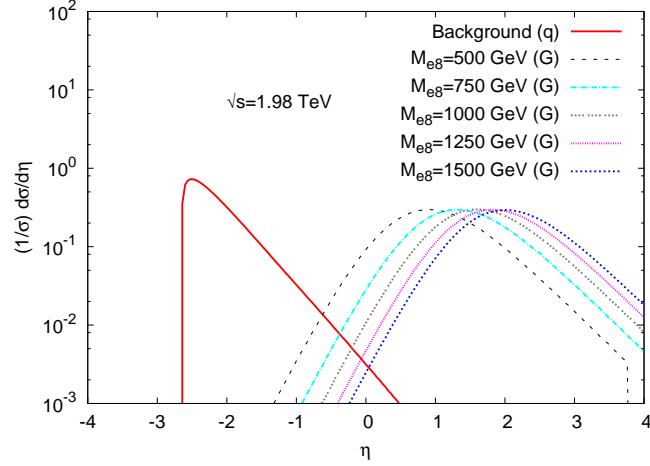


Figure 10: Pseudo-rapidity distributions of jets for signal and background at $\sqrt{s} = 1.98$ TeV and $\Lambda = 10$ TeV.

The numbers of signal and background events for 6 different M_{e8} values are presented in Table 4 (the mass window used is the same as the one used in previous subsection). As seen from the Table very clean signal can be obtained up to $M_{e8} \simeq 1500$ GeV.

Reachable Λ scales for 5 different mass values are given Table 5. Comparison with Table 3 show that twofold increasing of the electron energy results in: 1.5 times higher values of Λ for $M_{e8} = 500$ GeV, 2 times - for $M_{e8} = 750$ GeV and 4 times - for $M_{e8} = 1000$ GeV. Moreover, multi-ten TeV scales can be achieved for $M_{e8} = 1250$ and 1500 GeV, which are not available at LHeC/QCDE-1.

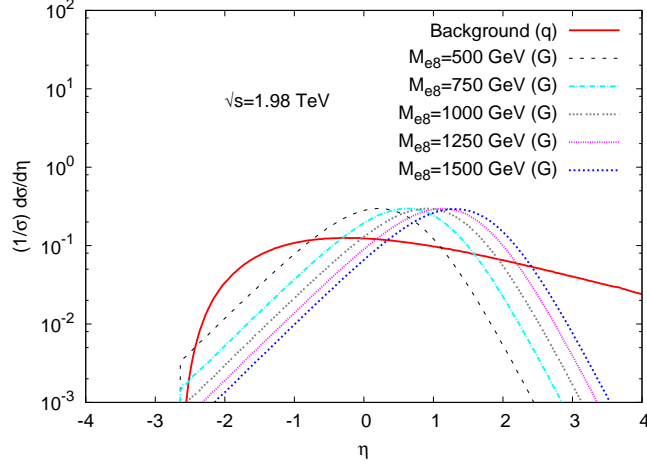


Figure 11: Pseudo-rapidity distributions of electrons for signal and background at $\sqrt{s} = 1.98$ TeV and $\Lambda = 10$ TeV.

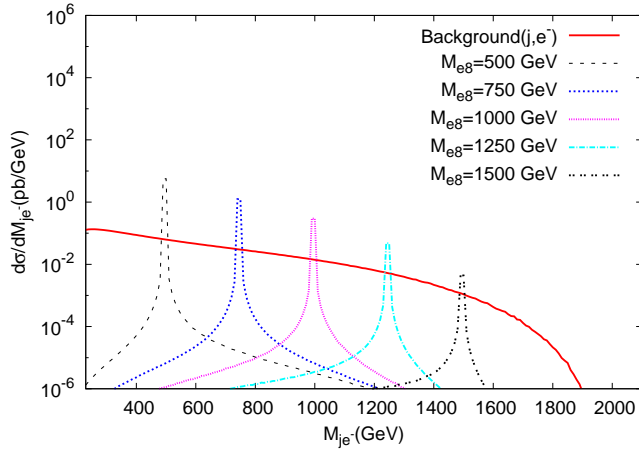


Figure 12: ej invariant mass distributions for signal and background at $\sqrt{s} = 1.98$ TeV and $\Lambda = 10$ TeV.

Finally, for a given $L_{int} = 1 fb^{-1}$, the upper mass limits for 5σ discovery at LHeC/QCDE-2 are $M_{e8} = 1580$ GeV and $M_{e8} = 1775$ GeV for $\Lambda = 10$ TeV and $\Lambda = M_{e8}$, respectively.

M_{e8} , GeV	$\Lambda = M_{e8}$		$\Lambda = 10$ TeV	
	S	B	S	B
500	3.3×10^7	1.4×10^3	9.8×10^4	940
750	3.9×10^6	1000	2.6×10^4	445
1000	5.0×10^5	630	5.8×10^3	210
1250	5.3×10^4	270	980	76
1500	3.5×10^3	77	89	16
1750	55	6	2	1

Table IV: Number of signal and background events for LHeC/QCDE-2 with $L_{int} = 1fb^{-1}$.

M_{e8} , GeV	$L_{int} = 1fb^{-1}$	$L_{int} = 10fb^{-1}$
500	245 (320)	440 (570)
750	150 (195)	275 (355)
1000	82 (110)	155 (205)
1250	41 (56)	81 (107)
1500	16 (23)	34 (46)

Table V: Achievable compositeness scale (Λ in TeV units) at LHeC/QCDE-2 for 5σ (3σ) statistical significance.

IV. CONCLUSION

It seems that QCD Explorer stage(s) of the LHeC, together with providing necessary information on PDF's and QCD basics, could play essential role on the BSM physics, also. Concerning color octet electrons. LHeC/QCDE-1 will cover M_{e8} mass up to O(1200 GeV), whereas LHeC/QCDE-2 will enlarge covered mass range up to O(1700 GeV).

The discovery of e_8 at this machine, simultaneously will determine compositeness scale. For example, if $M_{e8} = 500$ GeV LHeC/QCDE-2 with $L_{int} = 10 fb^{-1}$ will be sensitive to Λ up to 570 TeV.

Acknowledgments

Authors are grateful to A. Celikel and M. Kantar for useful discussions. This work is supported by TUBITAK in the framework of the BIDEF post-doctoral program and TAEK under the grant No CERN-A5.H2.P1.01-11.

- [1] I.A.D' Souza, C.S. Kalman, PREONS: Models of leptons, quarks and gauge bosons as composite objects, World Scientific Publishing Co, 1992.
- [2] H. Harari, Phys. Lett. B 86 (1979) 83.
- [3] H. Fritzsch, G. Mandelbaum, Phys. Lett. B 102 (1981) 319.
- [4] O.W. Greenberg, J. Sucher, Phys. Lett. B 99 (1981) 339.
- [5] R. Barbieri, R.N. Mohapatra, A. Maseiro, Phys. Lett. B 105 (1981) 369.
- [6] U. Baur, K.H. Streng, Phys. Lett. B 162 (1985) 387.
- [7] A. Celikel, M. Kantar, S. Sultansoy, Phys. Lett. B 443 (1988) 359.
- [8] G. Amsler *et al.* (Particle Data Group), Phys. Lett. B 667 (2008) 1.
- [9] F. Abe *et al.*, Phys. Rev. Lett. 63 (1989) 1447.
- [10] J.L. Hewett, T.G. Rizzo, Phys. Rev. D 56 (1997) 9.
- [11] I. Abt *et al.*, Nucl. Phys. B 396 (1993) 3; T. Ahmed *et al.*, Z. Phys. C 64 (1994) 545.
- [12] S. Sultansoy, Eur. Phys. J. C 33 (2004) S1064.
- [13] S. Sultansoy, in: Proceedings of Particle Accelerator Conference, Knoxville, 2005, p. 4329.
- [14] A.N. Akay, H. Karadeniz, S. Sultansoy, arXiv:0911.3314 [physics.acc-ph].
- [15] The LHeC web page, <http://www.lhec.org.uk>.
- [16] J.B. Dainton *et al.*, JINST 1 (2006) P10001.
- [17] D. Schulte, F. Zimmerman, in: Proceedings of European Particle Accelerator Conference, Lucerne, Switzerland, 2004, p. 632.
- [18] H. Karadeniz, S. Sultansoy, in: Proceedings of European Particle Accelerator Conference, Edinburgh, 2006, p. 673.
- [19] F. Zimmerman *et al.*, in: Proceedings of European Particle Accelerator Conference, Genoa, Italy, 2008, p. 2847.
- [20] A. Celikel, M. Kantar, Tr. J. of Phys. 22 (1998) 401.

- [21] A. Pukhov, et al., hep-ph/9908288.
- [22] D. Stump, et al., JHEP 0310 (2003) 046.